HHS Public Access

Author manuscript

Heart Rhythm. Author manuscript; available in PMC 2016 June 14.

Published in final edited form as:

Heart Rhythm. 2015 January ; 12(1): 211–219. doi:10.1016/j.hrthm.2014.09.051.

Novel Timothy Syndrome Mutation Leading to Increase in *CACNA1C* Window Current

Nicole J. Boczek, BA[1,2,*], **Erin M. Miller, MS, LCGC**[3,*], **Dan Ye, MD**[4,*], **Vlad V. Nesterenko, PhD**[5], **David J. Tester, BS**[4], **Charles Antzelevitch, PhD, FACC, FAHA, FHRS**[5], **Richard J. Czosek, MD**[3], **Michael J. Ackerman, MD, PhD**[4,6,7], and **Stephanie M. Ware, MD, PhD**[8]

[1]Center for Clinical and Translational Science, Mayo Clinic, Rochester, MN, 55905, USA

[2]Mayo Graduate School, Mayo Clinic, Rochester, MN, 55905, USA

[3]The Heart Institute, Cincinnati Children's Hospital Medical Center, Cincinnati, OH, 45229, USA

[4]Department Molecular Pharmacology & Experimental Therapeutics, Windland Smith Rice Sudden Death Genomics Laboratory, Mayo Clinic, Rochester, MN, 55905, USA

[5]Department of Pharmacology, Masonic Medical Research Laboratory, Utica, NY, 13501

[6]Department of Medicine (Division of Cardiovascular Diseases), Mayo Clinic, Rochester, MN, 55905, USA

[7]Department of Pediatrics (Division of Pediatric Cardiology), Mayo Clinic, Rochester, MN, 55905, USA

[8]Departments of Pediatrics and Medical and Molecular Genetics, Indiana University School of Medicine, Herman B. Wells Center for Pediatric Research, Indianapolis, IN, 46202, USA

Abstract

Correspondence: Michael J. Ackerman, Mayo Clinic Windland Smith Rice Sudden Death Genomics Laboratory, Guggenheim 501, Mayo Clinic, 200 First Street SW, Rochester, MN 55905, 507-284-0101 (phone), 507-284-3757 (fax), ackerman.michael@mayo.edu, Stephanie M. Ware, Indiana University School of Medicine, 1044 W Walnut R4-227, Indianapolis, IN 46202, 317-274-8938, stware@iu.edu.

*Each of these authors contributed equally to this manuscript

Conflicts of Interest:

The other authors have no conflicts of interest relevant to this article to disclose.

Contributor's Statement:

Nicole J. Boczek: Ms. Boczek aided in experimental analysis, drafted the manuscript, and approved the final manuscript.
Erin M. Miller: Ms. Miller aided in the patient's care, and reviewed, revised, and approved the final manuscript.
Dan Ye: Dr. Ye aided in experimental design, carried out experimental analysis, and reviewed, revised, and approved the final manuscript.
Vlad V. Nesterenko: Dr. Nesterenko completed modeling studies, and reviewed, revised, and approved the final manuscript.
David J. Tester: Mr. Tester aided in experimental design, and reviewed, revised, and approved the final manuscript.
Charles Antzelevitch: Dr. Antzelevitch aided in modeling studies, and reviewed, revised, and approved the final manuscript.
Richard J. Czosek: Dr. Czosek cared for the patient, reviewed, revised, and approved the final manuscript.
Michael J. Ackerman: Dr. Ackerman aided in experimental design, and reviewed, revised, and approved the final manuscript.
Stephanie M. Ware: Dr. Ware cared for the patient, aided in experimental design, and reviewed, revised, and approved the final manuscript.

Background—Timothy syndrome (TS) is a rare multi-system genetic disorder characterized by a myriad of abnormalities including QT prolongation, syndactyly, and neurological symptoms. The predominant genetic causes are recurrent *de novo* missense mutations in exon 8/8A of the *CACNA1C*-encoded L-type calcium channel, however some cases remain genetically elusive.

Objective—To identify the genetic cause of TS in a case that did not harbor a *CACNA1C* mutation in exon 8/8A, and was negative for all other plausible genetic substrates.

Methods—Utilization of diagnostic exome sequencing to identify the genetic substrate responsible for our case of TS. The identified mutation was characterized using whole cell patch-clamp technique and the results of these analyses were modeled using a modified Luo-Rudy dynamic model to determine the effects on the cardiac action potential.

Results—Whole exome sequencing revealed a novel *CACNA1C* mutation, p.Ile1166Thr, in a young male with diagnosed TS. Functional electrophysiological analysis identified a novel mechanism of TS-mediated disease, with an overall loss of current density and a gain-of-function shift in activation, leading to an increased window current. Modeling studies of this variant predicted prolongation of the action potential, as well as the development of spontaneous early afterdepolarizations.

Conclusion—Through expanded whole exome sequencing, we have identified a novel genetic substrate for TS, p.Ile1166Thr-CACNA1C. Electrophysiological experiments combined with modeling studies have identified a novel TS mechanism through increased window current. Therefore, expanded genetic testing in cases of TS to the entire *CACNA1C* coding region, if initial targeted testing is negative, may be warranted.

Keywords

Timothy Syndrome; *CACNA1C*; Window Current; Genetics; Whole Exome Sequencing

INTRODUCTION

Timothy syndrome (TS), an extremely rare genetic disorder with less than 30 cases reported worldwide, is characterized by a myriad of multisystem abnormalities including QT prolongation, syndactyly, congenital heart defects, facial dysmorphisms, and neurological symptoms including autism, seizures, and intellectual disability.[1, 2] Due to extreme QT prolongation, these individuals can experience ventricular fibrillation and cardiac arrest, and the overall compilation of multisystem abnormalities often leads to early demise around 2.5 years of age, however in rare cases affected individuals have survived beyond childhood.[3]

The predominant genetic cause, identified in 2004, was a recurrent *de novo* heterozygous missense mutation, p.Gly406Arg, in the alternatively spliced exon 8 (exon 8A) in the *CACNA1C*-encoded L-type calcium channel (LTCC).[1] Following the original genetic discovery of a mutational hot spot within exon 8A, two additional mutations were identified in exon 8, p.Gly406Arg and p.Gly402Ser. Exons 8 and 8A undergo alternative splicing in a mutually exclusive manner, with exon 8 being the predominantly expressed isoform.[4] It has been suggested that mutations in exon 8 result in a slightly different phenotype than the p.Gly406Arg mutation in exon 8A. For example, the two patients with exon 8 mutations

were not reported to have syndactyly, emphasizing the variability of the phenotypic manifestation of TS. Unlike other channelopathies, where mutational "hot-spots" are rare, these three missense mutations make up almost all of published TS cases and confer the same impaired open-state voltage dependent inactivation. The mutation clustering has led to targeted genetic screening for suspected TS, focusing specifically on exon 8/8A and surrounding regions within the *CACNA1C* gene.

Here, we have described a novel *CACNA1C* mutation that was identified via whole exome sequencing (WES), outside of the canonical exon 8/8A region of the channel in exon 27, in a patient exhibiting a TS phenotype with QT prolongation, patent ductus arteriosis, seizures, facial dysmorphisms, joint hypermobility, hypotonia, hand anomalies (clinodactyly and short thumbs), intellectual impairment, and tooth decay. Interestingly, patch clamp analysis identified a novel electrophysiological phenotype, distinct from the loss of inactivation seen in the previously established TS genotypes.

METHODS

Study Subject

The patient was seen at Cincinnati Children's Hospital Medical Center (CCHMC). CCHMC's IRB does not require consent for single patient studies, and the patient is deceased. In addition, genetic testing completed on the patient was done as part of a clinical genetics evaluation, and was approved by the patient's family. All other research based questions completed in the manuscript did not utilize patient materials.

HEK293 Cell Culture and Transfection

Details regarding the constructs and HEK293 cell culture are described in the supplement. Heterologous expression of $Ca_v1.2$ was accomplished by cotransfecting 1 μg *CACNA1C* wild type (WT) or mutant (Ile1166Thr-CACNA1C) cDNA with 1 μg *CACNB2b*, 1 μg *CACNA2D1* and 0.25 μg Green Fluorescence Protein (GFP) cDNA with the use of 9μl Lipofectamine 2000. The media was replaced with OPTI-MEM after 4–6 hours. Transfected cells were incubated for 48 hours before electrophysiological experiments.

Electrophysiological Measurements

Standard whole-cell patch clamp technique was used to measure I_{CaL} wild type and mutant calcium currents at room temperature (22–24°C) using methods provided in the supplement.

Statistical Analysis

All data points are shown as the mean value and error bars represent the standard error of the mean. A Student's t-test was performed to determine statistical significance between two groups. A $P<0.05$ was considered to be significant.

Simulated L-type Calcium Current and Ventricular Action Potentials

In order to simulate possible effects of the heterozygous p.Ile1166Thr mutation in the *CACNA1C* gene on the cardiac action potential, we used the dynamic Luo-Rudy model[5]

with subsequent adjustments as implemented by Faber and Rudy (LR2).[6–8] Additional information regarding this model and how it was applied is available in the supplement.

RESULTS

Clinical Description and Genetic Testing

The proband was born to a healthy 38-year-old female and 35-year-old male both of Caucasian descent. There was no report of consanguinity and the family histories were non-contributory. The pregnancy was uncomplicated. Birth weight was 3.5 kg (50th centile), length was 47 cm (10th centile) and head circumference measured 35 cm (35th centile). He was transferred from the birth hospital on the first day of life for further evaluation of bradycardia, later diagnosed as 2:1 atrioventricular (AV) conduction. The patient remained hospitalized for 6 weeks. Initial cardiac evaluation revealed 2:1 AV block (Figure 1A) and marked ventricular repolarization delay with QT interval prolongation measurement ranging from 595 to 812 milliseconds (ms). Medical therapy (propranolol) was initiated and QTc duration stabilized (550–650 ms). With beta-blockade, 2:1 AV conduction resolved and there was consistent 1:1 AV conduction with significant T-wave alternans (Figure 1B). Initial imaging with echocardiogram demonstrated a patent ductus arteriosis (PDA) and left atrial enlargement.

The baby underwent automatic implantable cardioverter-defibrillator (ICD) placement, left sympathectomy and PDA ligation at one month of age. On the day of device implant, he received inappropriate defibrillator discharges secondary to T-wave oversensing and the device therapies were turned off. Defibrillator event monitoring was turned on after computerized theoretical T-wave shock avoidance was performed[9] and therapies were reinstated after multiple days with no theoretical shock being delivered. He presented at 5 weeks of age with desaturations and increased respiratory distress and was diagnosed with biventricular dysfunction and pulmonary hypertension of unclear etiology.

At 7 months of age he was found to have severe asymmetric septal hypertrophy with the intraventricular septum measuring 1.60 cm (z score 7.59), left ventricular diastolic dimension measuring 2.00 cm (z score −3.72), and left ventricular free wall measuring 0.40 cm (z score of −0.08). There was no evidence of left ventricular outflow tract obstruction. Although the etiology of hypertrophy is unclear, it resolved with discontinuation of corticosteroids and a change in antiepileptic medication. The last echocardiogram completed at 3 years 8 months of age demonstrated normal cardiac size, thickness and function.

In addition to prolonged QT, the patient also had a history of seizures. He developed infantile spasms at 5 months of age and was started on medical therapy. He then developed apneic seizures with both seizure types being difficult to control. He was started on a ketogenic diet at 10 months of age resulting in excellent seizure control. Brain CT showed progressive cerebral and cerebellar atrophy over the next 18 months (Figure 1C). In addition, the patient developed intractable irritability of unclear etiology despite extensive evaluations and management by the pain team.

On physical examination the patient had facial dysmorphisms with hypertelorism, flattened nasal bridge, short nose, prominent forehead, small tented mouth, hypotonic facies and sparse hair. He had joint hypermobility including the fingers, dimpling at the elbow and shoulder joints, clinodactyly (Figure 1D), short thumbs, bilateral metatarsus adductus, osteopenia (Figure 1E), hypotonia, and unilateral cryptorchidism. In addition, the patient had severely hypoplastic teeth and decay, and at 2 years 7 months of age had extraction of 20 teeth.

An extensive diagnostic work-up was completed in an attempt to identify an underlying, unifying diagnosis. The following tests were completed in CLIA-certified clinical genetic testing laboratories and were normal: Long QT syndrome (LQTS) gene panel (*KCNQ1, KCNH2, SCN5A, KCNE1, KCNE2, KCNJ2, CACNA1C* (exons 8, 8A, and 9), *CAV3, SCN4B, AKAP9* (exon 18), *SNTA1*), chromosome SNP microarray, routine chromosome analysis, and sequencing of *MECP2, MEF2C, CDKL5, FOXG1, ARX, SCO2, SURF1, FASTKD2, COX10, COX15, SCO1* and *COX6B1*. Deletion/duplication testing was also completed for *MECP2, MEF2C, CDKL5,* and *ARX*.

Twenty-four genes associated with congenital disorders of glycosylation (CDG) were sequenced and a missense mutation was identified in the *PMM2* gene, c.590A>C (p.E197A). Given the autosomal recessive mode of inheritance of CDG, deletion/duplication analysis of the same 24 genes was completed and a second mutation was not identified.

Given prior negative genetic testing and a likely genetic etiology, WES through a commercial genetic testing laboratory was requested when this testing became clinically available. A novel missense variant (c. 3497T>C; p.Ile1166Thr) in exon 27 of the *CACNA1C* gene was identified (Figure 2). The amino acid is completely conserved throughout vertebrates and is predicted to be probably damaging and deleterious by *in silico* analysis. The variant is located outside of the canonical TS mutation region in *CACNA1C* and the position was not evaluated on the LQTS gene panel previously completed. The variant was confirmed with Sanger sequencing and co-segregation analysis showed that the patient's mother and father did not carry the variant, indicating a *de novo* variant occurrence. The variant was interpreted as disease causing and the patient was given a diagnosis of TS. WES did not identify any other primary childhood onset disease associated mutations.

The patient had multiple admissions for respiratory failure often associated with profound stooling and dehydration. Despite numerous medical interventions, the child ultimately died at 3 years 8 months of age after an admission for respiratory failure, hypotension, and dehydration. Prior to his death, he had only a single episode of polymorphic ventricular tachycardia that was non-sustained and did not meet duration criteria for device intervention.

Electrophysiological Based Studies of p.Ile1166Thr

Functional testing of the p.Ile1166Thr mutation identified in the patient was undertaken in order to better delineate the mechanism underlying the phenotypic features distinct from classic TS. Typical I_{CaL} tracings of voltage-dependent activation for WT and Ile1166Thr are shown in Figure 3A (see inset Figure 3A and figure legend). Analysis of the current-voltage relationship shows that the Ile1166Thr mutant shifted peak current from +30 mV (WT) to

+20 mV and dramatically reduced current density at +30 mV by 46.6% from −46.6 ± 8.0 picoamps/picofarad (pA/pF) (WT, n=11) to −24.9 ± 5.6 pA/pF (Ile1166Thr, n=11, $P<0.05$), indicating a marked loss-of-function electrophysiological phenotype (Figure 3B). A plot of activation curves shows that the Ile1166Thr mutation shifted $V_{1/2}$ of activation to less depolarized potential by −8.4 mV from 15.9 ± 1.7 mV (WT, n=11) to 7.5 ± 1.6 mV (Ile1166Thr, n=11; $P<0.05$; Figure 4A), indicating a significant decrease in the degree of depolarization required for activation of Ile1166Thr-containing channels and gain-of-function electrophysiological phenotype. The respective k (slope factor) showed no significant difference, changing from 6.9 ± 0.7 (WT, n=11) to 5.5 ± 0.9 (Ile1166Thr, n=11; $P>0.05$). In addition, there was a marked shift in the reversal potential of 78.2 ± 1.6 mV (n=11) for CACNA1C-WT, and 70.0 ± 2.0 mV (n=11) for CACNA1C-Ile1166Thr.

Steady-state inactivation was assessed by a standard two-pulse voltage-clamp protocol (see inset Figure 4B and figure legend). There was not a significant shift in $V_{1/2}$ of inactivation when comparing WT (−27.8 ± 1.8 mV; n=10) to the mutant Ile1166Thr (−30.6 ± 2.4 mV; n=4; $P>0.05$; Figure 4B). The respective k slope factor also remained unchanged at 10.6 ± 0.9 (WT, n=10) and at 7.8 ± 1.0 (Ile1166Thr, n=4; $P>0.05$). In order to better examine the increased window currents, the activation and inactivation curves were plotted together in Figure 4C–D.

I_{CaL} decay after 90% of peak was best fit by the two exponential equation with two τ values representing fast and slow inactivation. At 0 mV, Ile1166Thr mutant I_{CaL} revealed a faster inactivation τ in fast component of the decay time ($P<0.05$; Figure 4E). Slow inactivation τ remained unchanged (Figure 4F).

Modeling Studies of p.Ile1166Thr

In order to better understand the effect that the *CACNA1C*-Ile1166Thr mutation may play on cardiac action potential, we utilized a modified Luo-Rudy dynamic model.[6–8] At first, we determined the modifications of the intrinsic properties of the original I_{CaL} model that most accurately reproduce the behavior of the mutant Ile1166Thr I_{CaL} during the same voltage clamp protocols as were employed experimentally (see Supplementary Material for details). These preliminary simulations showed that the accurate behavior of the Ile1166Thr mutant I_{CaL} can be simulated by shifting the intrinsic steady-state activation by −14.1 mV towards more negative potentials and by decreasing the slope of the activation curve by the factor of 0.83 without any changes in the voltage-dependence of the activation time constant. The parameters describing the inactivation process were the same for both WT and Ile1166Thr mutant I_{CaL}. In addition, the maximal conductance of Ile1166Thr mutant channels was decreased to 33% of the WT (original) I_{CaL} model. Theoretical steady-state activation and inactivation curves, which were used to simulate WT and Ile1166Thr mutant I_{CaL} in Luo-Rudy model of the action potential, are shown on Figure 5A.

According to this model, there may be a considerable overlap between the steady-state activation and inactivation curves, resulting in a substantial steady-state (“window”) calcium current that peaks around −20 mV which is increased by the negative shift of the steady-state activation curve approximately 2.5 times (Figure 5B). In addition, the negative shift in the

steady-state activation/deactivation curve will result in delayed deactivation of the calcium current, which will occur at more negative voltages during the action potential.

Figure 5C shows the effect of the heterozygous expression (50% WT + 50% mutant) of the Ile1166Thr mutation on the shape and duration of simulated APs. The Ile1166Thr mutation resulted in a prolongation of the action potential duration (APD90) by 21% (from 165.0 ms to 200.0 ms) at constant basic cycle length (BCL) of 1000 milliseconds. The peak of the calcium transient during the action potential with the simulated heterogeneous expression of Ile1166Thr mutation was 97% of that of the WT I_{CaL}(Figure 5D), indicating no significant change in the total calcium influx.

Figure 5E illustrates the time course of the calcium current during the action potential for WT and heterozygously expressed Ile1166Thr mutant. Note that the peak of I_{CaL} and its first late components are substantially decreased due to the mutation, but the second late component appears at more negative potentials due to the failure of the mutant I_{CaL} to deactivate. The abnormal shape of the I_{CaL} time course due to the mutation is more evident in Figure 5F, which shows the two components (WT and Ile1166Thr mutant) of I_{CaL} comprising of heterogeneously expressed mutant current. The mutant channel displays a much delayed late component due to the more negative deactivation of the persistent (window) component of the current.

Finally, the model predicts that the Ile1166Thr-mutation of CACNA1C may result in a substantial instability of action potential (AP) after a prolonged pause. Figure 5G shows that the omission of one beat (2000 ms pause) leads to early afterdepolarizations (EADs) evident on AP simulated with 50% of Ile1166Thr-mutant I_{CaL}, which is absent in AP simulated with WT I_{CaL}.

DICUSSION

WES is useful for identification of genetic etiology in patients with rare disorders, non-classic phenotypes, and novel syndromes. In this study, we identified a patient with multiple abnormalities including QT prolongation. While he shared many features of TS, he also had some atypical anomalies, and sequencing of the TS canonical region with a LQTS panel did not identify any genetic abnormalities. WES results suggest that a novel *de novo* mutation in *CACNA1C*, outside the canonical TS region, explains his phenotype, and the distinct results obtained with functional analyses highlight a novel mechanism.

In order to confirm the disease-causing nature of this mutation and further investigate mechanism of action, heterologous expression of the LTCC was utilized to examine the electrophysiological properties using whole cell patch clamp technique. These analyses of p.Ile1166Thr led to an unexpected, distinct electrophysiological phenotype from the classical TS mutations. Electrophysiological studies of p.Gly406Arg in exon 8A and p.Gly406Arg and p.Gly402Ser in exon 8 were originally completed in heterologous over-expression systems, and identified that these mutations lead to almost complete loss of inactivation of $Ca_v1.2$.[1, 4] In addition, p.Gly406Arg in exon 8 or 8A also leads to slight negative shifts in the voltage dependence of activation.[1, 4] Conversely, p.Ile1166Thr leads to

an overall loss of current density and a gain-of-function shift in activation leading to an increased window current. Increased window currents in $Ca_v1.2$ have been attributed to electrophysiological based cardiac diseases and have been suggested to play a major role in the initiation of early afterdepolarizations (EADs),[10, 11] but have not previously been associated with a TS phenotype.

Due to the differing electrophysiological phenotypes between the canonical p.Gly406Arg/p.Gly402Ser mutations and p.Ile1166Thr, we performed modeling studies to better understand how the increased window current resulting from the p.Ile1166Thr mutation may affect the cardiac action potential. Like the modeling studies completed for p.Gly406Arg/p.Gly402Ser,[1, 4] our simulations predict similar prolongation of the action potential (17% due to Gly406 vs. 21% due to Ile1166Thr) as well as the development of spontaneous EADs, which can lead to ventricular fibrillation and sudden death. Modeling studies in exon 8A p.Gly406Arg-mediated TS have been validated previously through electrophysiological characterization of the prolonged action potential of human iPSC derived cardiomyocytes,[12] confirming the accuracy of the modeling studies in predicting the effects of this mutation in a human cardiomyocyte model.

In addition, this mutation, p.Ile1166Thr, has not been previously identified in the publically available online databases, including the 1000 Genomes Project (n=1,092; http://browser.1000genomes.org/index.html) or the NHLBI Exome Sequencing Project (n=6,503; http://evs.gs.washington.edu/EVS/) emphasizing its rarity. After co-segregation analysis with the parents of the child, it was determined that this mutation was sporadic, which is the typical mode of inheritance for TS. Therefore, the combination of the rarity of this mutation, its *de novo* presentation, the electrophysiological phenotype, and our modeling studies gives sufficient evidence to support that p.Ile1166Thr is indeed the cause of the prolonged QT intervals, and likely the TS phenotype observed in our patient.

TS was initially characterized by QT prolongation and syndactyly associated with the p.Gly406Arg mutation.[1] When two additional individuals with a TS phenotype were identified with mutations located in exon 8 (p.Gly406Arg and p.Gly402Ser) without syndactyly and a more severe cardiac phenotype compared to the exon 8A mutation, it was suggested that this may be another form of the condition (TS2).[4] Additional novel phenotypes included hyper-flexible joints and hypotonia,[4] which were also observed in our patient. A fourth mutation (p.Ala1473Gly; Figure 2) was identified in an individual with features suggestive of TS. Interestingly, this patient had somewhat more severe phenotypic features, similar to our patient, including dysmorphic features, seizures, 2:1 AV block, QT interval prolongation, and profound developmental delay.[13] Although extracardiac differences in phenotype have been observed across all of the mutations, the cardiac phenotype does appear consistent with QT prolongation, arrhythmias, cardiac hypertrophy and PDA being commonly observed. The phenotypic differences observed with each mutation may represent variable expressivity as opposed to distinct disease types as previously suggested. The variation may also suggest potential genotype-phenotype correlations which cannot be fully elucidated based on the small number of affected individuals and *CACNA1C* mutations identified to date.

Novel Mechanisms of CACNA1C-Mediated Clinical Phenotypes

Patch clamp and modeling studies focus primarily on how these mutations lead to the cardiac phenotype of QT prolongation in these patients. However, there have been limited studies regarding the extra-cardiac phenotypes of TS mutations. It has been hypothesized that this loss of inactivation is detrimental to the proper function of the *CACNA1C*-encoded channel, and is also responsible for the neuronal and skeletal phenotypes seen in TS.[1, 4] Conversely, we have now observed increased window current in $Ca_V1.2$ in a patient with TS. Therefore, a paradox emerges as to what the cause of the other multisystem phenotypes may be, and why these patients, with differing electrophysiological characteristics of the calcium channel, lead to a similar TS phenotype.

One unique observation, as shown in Figure 2, highlights that p.Ile1166Thr, and the four additional TS-associated mutations to date have been identified at the very end of the last transmembrane segment or at the beginning of the InterDomain Linkers (IDL). The unique localization of each of these mutations to the last transmembrane segment/IDL of these repeats highlights the possibility that these regions within the channel have an important and similar function.

Recently, it has been proposed that the neurological phenotypes associated with TS may not be due to electrophysiological disturbances in I_{CaL}, rather, may be due to altered signaling cascades controlled by a binding partner within the last transmembrane spanning region/IDL of the first repeat. Krey and colleagues have identified that the p.Gly406Arg mutation leads to dendrite retraction, which could be responsible for the neurological phenotypes observed in TS.[14] Interestingly, the dendritic retraction is not due to the excessive Ca2+ influx, rather, through a Ca2+ independent mechanism involving Gem and RhoA signaling cascades. They found that TS-mutant $Ca_v1.2$ channels could not bind appropriately to Gem, leading to the hypothesis that this interaction is essential to prevent dendrite retraction.[14]

Based on these observations, we hypothesize that when $Ca_v1.2$ is folded into its three dimensional pore in the cellular membrane, Gem, in addition to binding to last transmembrane spanning region/IDL of the first repeat, may also be binding to the last transmembrane/IDLs between each of the repeats. Taken together, the neuronal TS phenotype may be due to the location of the mutation in these channels, rather than the mutation's electrophysiological sequelae. Not only is Gem expressed in cortical neurons, but is also known to be linked to signaling cascades in the cytoskeleton, which could be important for skeletal phenotypes seen in TS including syndactyly and other hand abnormalities.

In addition, it has been identified recently that gain-of-function *CACNA1C* mutations, specifically p.P857R, can lead to a LQTS phenotype distinct from TS.[15] This mutation was identified recently in a large pedigree of genotype negative individuals with LQTS without any other organ system abnormalities. The p.P857R mutation led to an increased current density of $Ca_v1.2$ through increased membrane expression.[15] This discovery, taken together with the Gem/RhoA signaling cascades mediated by $Ca_v1.2$, provides evidence that electrophysiological changes in $Ca_v1.2$ are likely responsible for the cardiac phenotype

while the extra-cardiac phenotypes may be due to signaling cascades distinct from electrophysiological channel abnormalities.

CONCLUSIONS

Through WES, we have identified a novel genetic substrate for TS, p.Ile1166Thr. Our electrophysiology studies identifying a novel mechanism of $Ca_v1.2$ dysfunction of increased window current in combination with our modeling studies have provided substantial evidence that p.Ile1166Thr could indeed lead to prolonged action potentials and possibly the other phenotypes observed in TS. Therefore, based on these studies, it may be warranted to expand genetic testing in patients with a TS-like phenotype to the entire *CACNA1C*-encoded L-type calcium channel if initial targeted testing of exon 8/8A return negative.

Supplementary Material

Refer to Web version on PubMed Central for supplementary material.

Acknowledgments

Michael J. Ackerman is a consultant for Boston Scientific, Gilead Sciences, Medtronic, and St. Jude Medical and receives sales based royalties from Transgenomic for their FAMILION-LQTS and FAMILION-CPVT genetic tests.

Funding Sources:

This work was supported by the Mayo Clinic Windland Smith Rice Comprehensive Sudden Cardiac Death Program, the Sheikh Zayed Saif Mohammed Al Nahyan Fund in Pediatric Cardiology Research, the Dr. Scholl Fund, and the Hannah M. Wernke Memorial Fund. In addition, N.J. Boczek was supported by an individual PhD predoctoral fellowship from the American Heart Association (12PRE11340005) and by CTSA Grant (UL1 TR000135) from the National Center for Advancing Translational Science (NCATS), a component of the NIH. Its contents are solely the responsibility of the authors and do not necessarily represent the official view of NIH.

Abbreviations

AP	Action potential
APD	Action potential duration
LR2	Adjusted Luo-Rudy Model
AV	Atrioventricular
BCL	Basic cycle length
CDG	Congenital disorders of glycosylation
I-V curve	Current-voltage curve
EADs	Early afterdepolarizations
EFFP	Enhanced yellow fluorescent protein
GFP	Green fluorescent protein
ICD	Implantable cardioverter-defibrillator

IDLs	InterDomain-linkers
LQTS	Long QT syndrome
LTCC	L-type calcium channel
ms	Milliseconds
mV	Millivolts
PDA	Patent ductus arteriosis
pA	Picoamps
pF	picofarads
TS	Timothy Syndrome
WES	Whole Exome Sequencing
WT	Wild-type

REFERENCES

1. Splawski I, Timothy KW, Sharpe LM, et al. Cav1.2 calcium channel dysfunction causes a multisystem disorder including arrhythmia and autism. Cell. 2004; 119:19–31. [PubMed: 15454078]
2. Krause U, Gravenhorst V, Kriebel T, Ruschewski W, Paul T. A rare association of long QT syndrome and syndactyly: Timothy syndrome (LQT 8). Clin Res Cardiol. 2011; 100:1123–1127. [PubMed: 21915623]
3. Splawski, I.; Timothy, KW.; Priori, SG.; Napolitano, C.; Bloise, R. Timothy Syndrome. In: Pagon, RA.; Adam, MP.; Ardinger, HH.; Bird, TD.; Dolan, CR.; Fong, CT.; Smith, RJH.; Stephens, K., editors. GeneReviews [Internet]. Seattle (WA): University of Washington, Seattle; 2006. [Updated 2011]
4. Splawski I, Timothy KW, Decher N, Kumar P, Sachse FB, Beggs AH, Sanguinetti MC, Keating MT. Severe arrhythmia disorder caused by cardiac L-type calcium channel mutations. PNAS. 2005; 102:8089–8096. [PubMed: 15863612]
5. Luo CH, Rudy Y. A dynamic model of the cardiac ventricular action potential. I. Simulations of ionic currents and concentration changes. Circ Res. 1994; 74:1071–1096. [PubMed: 7514509]
6. Zeng J, Laurita KR, Rosenbaum DS, Rudy Y. Two components of the delayed rectifier K+ current in ventricular myocytes of the guinea pig type. Theoretical formulation and their role in repolarization. Circ Res. 1995; 77:140–152. [PubMed: 7788872]
7. Zeng J, Rudy Y. Early afterdepolarizations in cardiac myocytes: mechanism and rate dependence. Biophys J. 1995; 68:949–964. [PubMed: 7538806]
8. Faber GM, Rudy Y. Action potential and contractility changes in Na+ overloaded cardiac myocytes: a simulation study. Biophys J. 2000; 78:2392–2404. [PubMed: 10777735]
9. Czosek RJ, Anderson JB, Cao J, Knilans TK. Assessment of T-wave oversensing in an infant with an implated defibrillator. Heart Rhythm. 2010; 7:1516–1517. [PubMed: 20493275]
10. Benitah JP, Alvarez JL, Gomez AM. L-type Ca2+ current in ventricular cardiomyocytes. J Mol Cell Cardiol. 2010; 48:26–36. [PubMed: 19660468]
11. Antoons G, Volders PGA, Stankovicova T, Bito V, Stengl M, Vos MA, Sipido KR. Window Ca2+ current and its modulation by Ca2+ release in hypertrophied cardiac myocytes from dogs with chronic atrioventricular block. J Physiol. 2007; 579:147–160. [PubMed: 17138604]

12. Yazawa M, Hsueh B, Jia X, Pasca AM, Bernstein JA, Hallmayer J, Dolmetsch RE. Using induced pluripotent stem cells to investigate cardiac phenotypes in Timothy syndrome. Nature. 2011; 471:230–234. [PubMed: 21307850]
13. Gillis J, Burashnikov E, Antzelevitch C, Blaser S, Gross G, Turner L, Babul-Hirji R, Chitayat D. Long QT, syndactyly, joint contractures, stroke and novel CACNA1C mutation: Expanding the spectrum of Timothy syndrome. Am J Med Genet A. 2012; 158A:182–187. [PubMed: 22106044]
14. Krey JF, Pasca SP, Shcheglovitov A, Yazawa M, Schwemberger R, Rasmusson R, Dolmetsch RE. Timothy syndrome is associated with activity-dependent dendritic retraction in rodent and human neurons. Nat Neurosci. 2013; 16:201–209. [PubMed: 23313911]
15. Boczek NJ, Best JM, Tester DJ, Giudicessi JR, Middha S, Evans JM, Kamp TJ, Ackerman MJ. Exome sequencing and systems biology converge to identify novel mutations in the L-type calcium channel, CACNA1C, linked to autosomal dominant long QT syndrome. Circ Cardiovasc Genet. 2013; 6:279–289. [PubMed: 23677916]

CLINICAL PERSPECTIVES

This report of a novel *CACNA1C* mutation, p.Ile1166Thr, expands the previously reported TS phenotype to include osteopenia, cerebral and cerebellar atrophy, intractable irritability, clinodactyly and short thumbs. While initial descriptions of TS suggest that syndactyly is a hallmark of the disorder, this and other reports encourage consideration of TS even in the absence of this finding. The difference in features reported in individuals with TS may represent variable expressivity as opposed to distinct disease types as previously suggested and may help inform genotype-phenotype correlations as additional mutations are identified and affected individuals are diagnosed. In addition, full sequencing of *CACNA1C* should be considered in individuals with negative sequencing of exons 8, 8A, and 9 if a diagnosis is suspected based on clinical presentation. Most clinical genetic testing laboratories offering a LQTS gene panel include *CACNA1C*, but some only sequence select exons thus missing potential disease causing mutations. Full sequencing of *CACNA1C* is available clinically as both a single gene test and part of larger LQTS gene panels and clinicians should be aware of the capabilities and limitations of genetic testing options. Clinicians can access a directory of international laboratories offering molecular genetic testing for LQTS and other disorders with links to clinical laboratories through Gene Tests, a medical genetics information resource developed for physicians, genetic counselors, other healthcare providers and researchers (http://genetests.org/tests/).

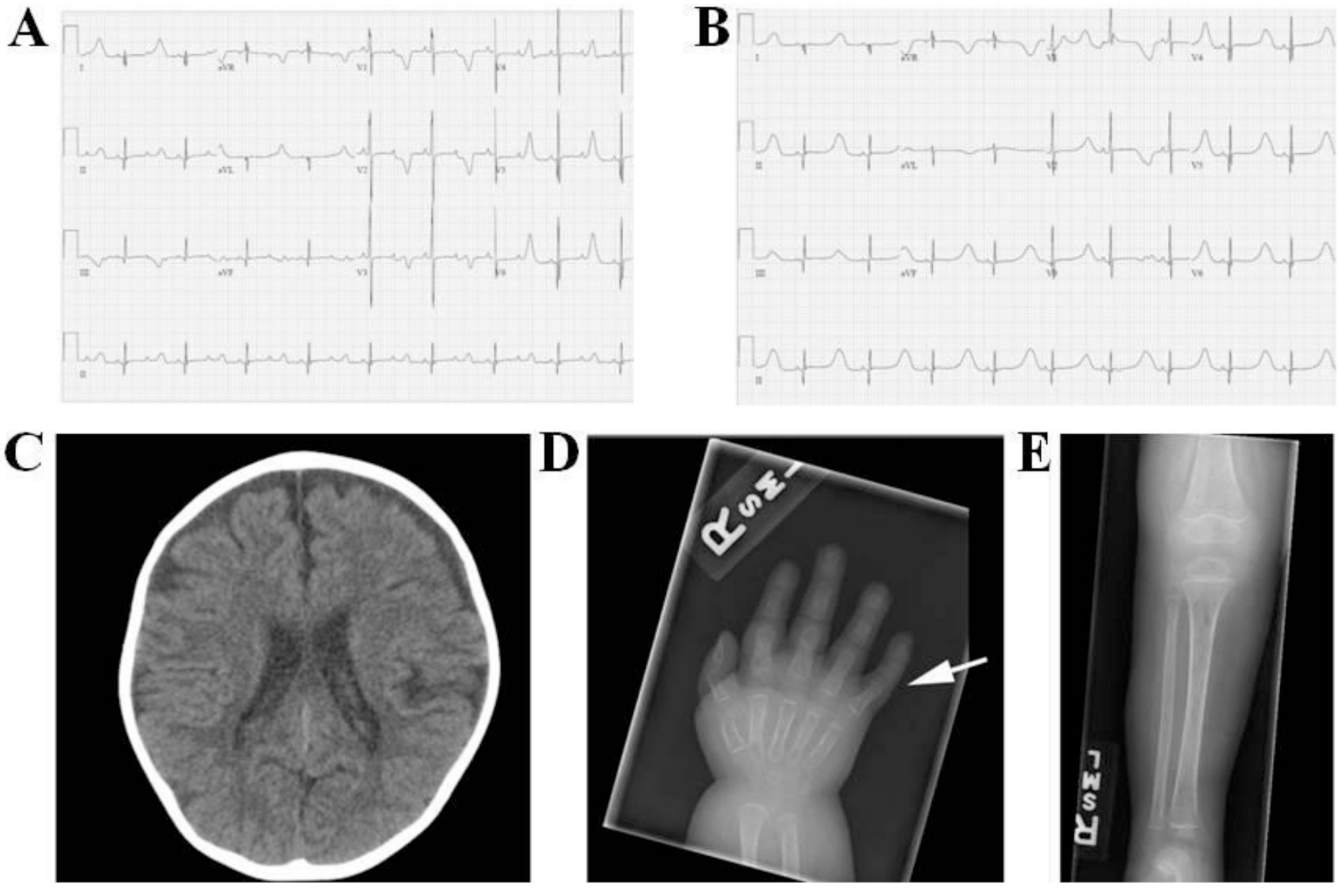

Figure 1. Electrocardiograms, CT Scan, and X-Ray Images from the Patient Harboring p.Ile1166Thr-CACNA1C

Electrocardiograms representing 2:1 block at birth **(A)** and t-wave alternans **(B)**. **(C)** Non-contrast CT of the head at 3 years 8 months of age showing mild diffuse cerebral parenchymal volume loss. **(D)** Right hand film at 10 months of age showing 5th finger clinodactyly (arrow). **(E)** AP tibia-fibula film at 10 months of age demonstrating osteopenia with a permeative appearance of the bone.

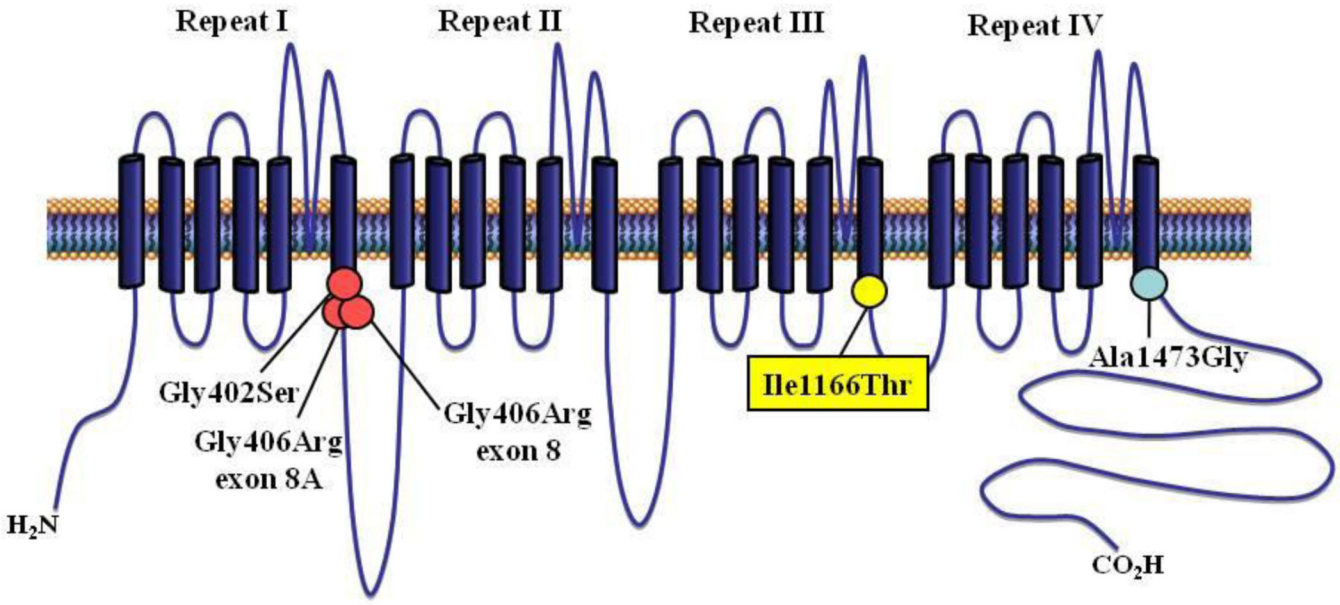

Figure 2. CACNA1C Protein Topology

Topology diagram of the CACNA1C channel α-subunit in the membrane. Each repeat is demarcated at the top of the figure. Red circles represent the canonical TS-associated mutations in exon 8 and 8A. The yellow circle represents the p.Ile1166Thr mutation identified within our patient. The blue circle represents the TS mutation identified by Gillis and colleagues.[13]

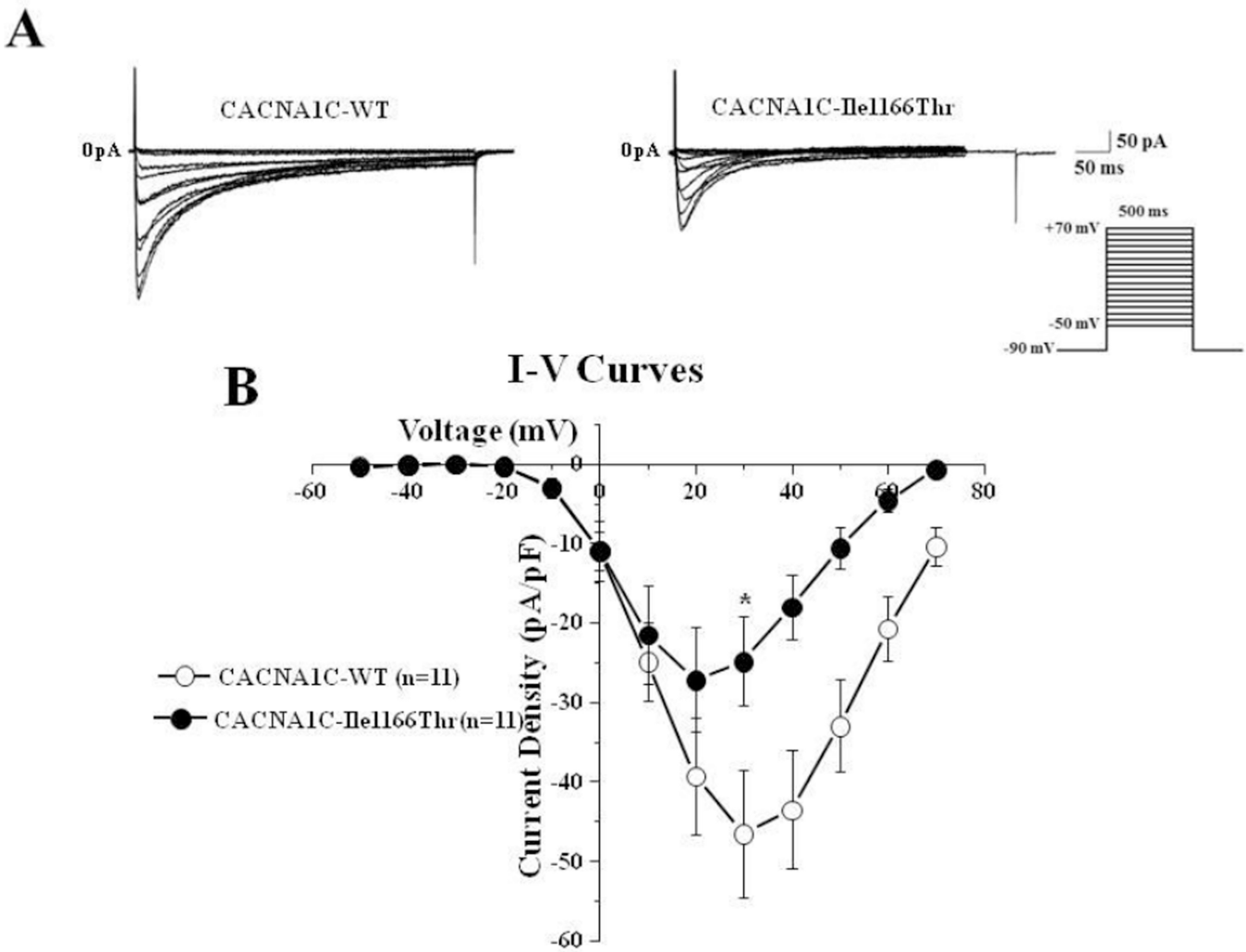

Figure 3. CACNA1C-Ile1166Thr Reduced I_{CaL} Current in Heterologous Cells

(A) Whole cell I_{CaL} current representative tracings from HEK293 cells expressing CACNA1C-WT or CACNA1C-Ile1166Thr determined from a holding potential of −90 mV to testing potential of +70 mV in 10 mV increments with 500 ms duration. **(B)** Current-voltage relationship for CACNA1C-WT (n=11) and –Ile1166Thr missense mutation (n=11). All values represent mean SEM. *p<0.05 vs. CACNA1C-WT.

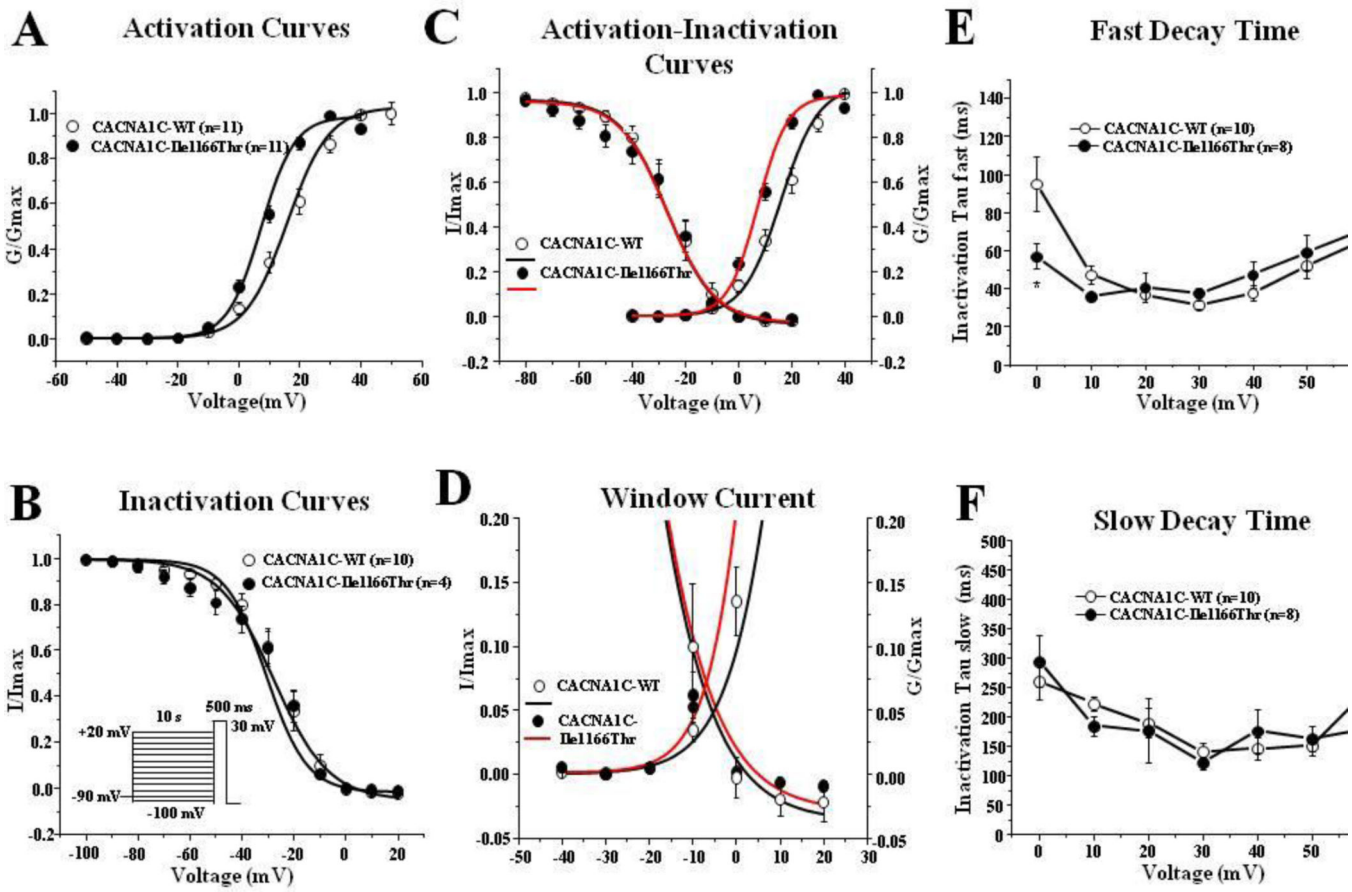

Figure 4. CACNA1C-Ile1166Thr Negatively Shifted I_{CaL} $V_{1/2}$ in Activation

(A) Activation curves of I_{CaL} CACNA1C-WT (n=11) and –Ile1166Thr mutation (n=11). G/Gmax represents normalized conductance fitted with a Boltzmann function. **(B)** Inactivation curves of I_{CaL} CACNA1C-WT (n=10) and Ile1166Thr variant (n=4), determined from a holding potential of −90 mV to pre-pulse of 20 mV in 10 mV increments with 10 s duration followed by a test pulse of 30 mV with 500 ms duration. I/Imax represent normalized calcium current fitted with a Boltzmann function. Plot **(C)** and magnified plot **(D)** of the activation and inactivation curves shown in panels A and B. **(E)** Inactivation time constants (τ) for the fast phase of I_{CaL} decay time of *CACNA1C*-WT (n=10) and Ile1166Thr variant (n=8) as a function of voltage. Time constants for each voltage step were determined by fitting a biexponential function to current decay. **(F)** Inactivation time constants (τ) for the slow phase of I_{CaL} decay time of CACNA1C-WT (n=10) and Ile1166Thr variant (n=8) as a function of voltage.

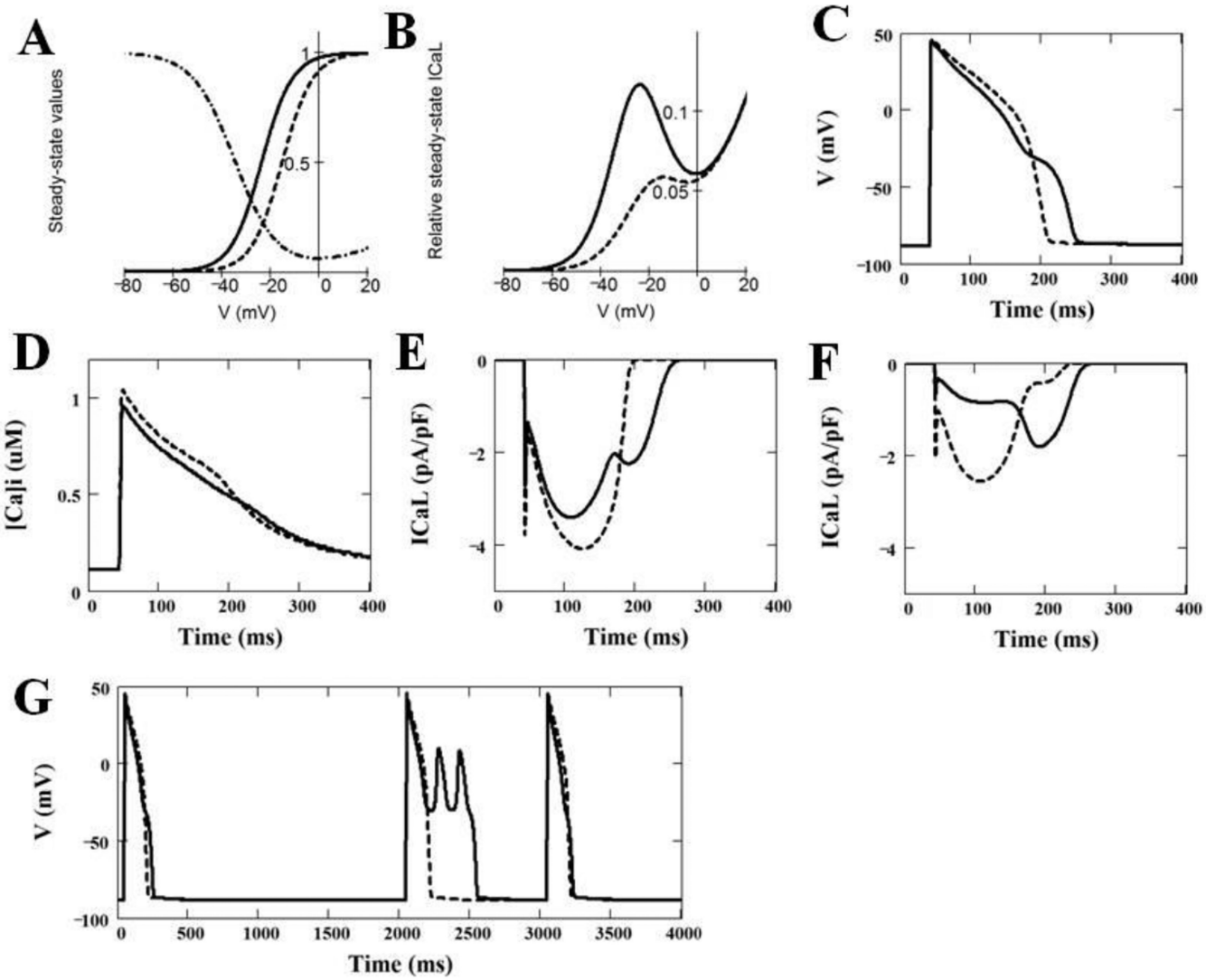

Figure 5. Simulation of Effects of CACNA1C-Ile1166Thr on the Properties of I_{CaL}, Cardiac Action Potential and Calcium Transients as Compared with WT-CACNA1C

(A) Intrinsic voltage-dependent activation and intrinsic voltage-dependent steady-state inactivation curves for WT I_{CaL} (dashed line) and Ile1166Thr mutant I_{CaL} (solid line). **(B)** Window I_{CaL} estimated theoretically as a product of the steady-state activation and the steady-state voltage-dependent inactivation curves for WT I_{CaL} (dashed curve) and for mutant I_{CaL} (solid curve). (**C**) Ventricular action potentials simulated by LR2 model using WT (dashed curve) and heterogeneously (50%/50%) expressed Ile1166Thr mutant (solid curve) I_{CaL} model. The panel shows 100th AP at BCL = 1000 ms. (**D**) Ca2+ transients, which correspond to the action potentials shown in panel C (solid line – WT; dashed line – 50% of Ile1166Thr mutant). (**E**) I_{CaL} during corresponding action potentials shown in panel C with WT (dashed line) and 50% of Ile1166Thr mutant (solid line) I_{CaL}; (**F**) Two components of I_{CaL} (shown by solid line in panel E) with 50% of Ile1166Thr mutant expression (dashed line – WT I_{CaL} component, solid line – Ile1166Thr I_{CaL} component).

(G) Effect of a missing beat on action potentials simulated using WT I_{CaL} (dashed line) and heterogeneously expressed mutant I_{CaL} (solid line).